Impacts of Aerosols on the Retreat of the Sierra Nevada Glaciers in California

Hesham El-Askary[1,2,3*], **Jingjing Li**[4], **Wenzhao Li**[1], **Thomas Piechota**[1], **Tommy Ta**[5], **Ariane Jong**[6], **Xinyi Zhang**[7], **Tiantian Yang**[8]

[1] *Schmid College of Science and Technology, Chapman University, CA 92866, USA*

[2] *Center of Excellence in Earth Systems Modeling and Observations, Chapman University, CA 92866, USA*

[3] *Department of Environmental Science, Faculty of Science, Moharam Beek, Alexandria University, Alexandria 21522, Egypt*

[4] *Department of Geosciences and Environment, California State University Los Angeles, CA 90032, USA*

[5] *Assistant Environmental Scientist/Engineer, CIM Group, CA 90010, USA*

[6] *Staff Scientist at Council for Watershed Health, CA 90012, USA*

[7] *China Petroleum Engineering and Construction Corporation (CPECC), Beijing 100120, China*

[8] *Department of Civil and Environmental Engineering, University of California Irvine, CA 92697, USA*

ABSTRACT

The snowpack in the Sierra Nevada mountain range is the primary source of water for California. Many studies have shown that the increase in aerosols could lead to a reduction of the snowpack in this region. This study focuses on evaluating changes in the snowpack during the winter and summer seasons from 2000 till 2016 and determining the relationship between aerosols and the retreat of glaciers in the Sierra Nevada. The change detection analysis has shown reductions of 76.4% and 91.4% in the snowpack during winter and summer, respectively. Utilizing the aerosol optical depth (AOD), Angstrom exponent, snow depth anomalies, snowfall, radiation fluxes, and albedo, the effect of aerosols on snowfall over the Sierra Nevada glaciers has been examined for this 17-year period. Overall, based on correlation analysis, a negative relationship exists between the AOD and the snowfall.

Keywords: Aerosols; Snowpack; Sierrea Nevada; Glacier Retreat.

INTRODUCTION

Many experiments have been conducted to see how global climate change has affected Earth's systems (Bolch, 2007). It was found that the changes in glaciers extent and/or retreat are key indicators of climate change (Irion, 2001; Kaser *et al.*, 2004). Changes to glacier's mass, volume, area, or length are clear signs, as they exhibit different levels of stress imposed by local climate causing the aforementioned glaciers' changes (Liu *et al.*, 2013). Due to the scarcity of ground measuring stations, satellite images proved to be more useful for analyzing long-term changes in glaciers (Prasad *et al.*, 2011). Change detection analysis has been applied in different ways to highlight temporal/spatial changes in different ecosystems (Bartsch *et al.*, 2010; El-Askary *et al.*, 2014).

The most common satellites used for analyzing glacier changes are Landsat satellites, equipped with powerful sensors such as Landsat Thematic Mapper (TM), Multispectral Scanner (MSS), Enhanced Thematic Mapper (ETM+), or Operational Land Imager (OLI), which have diverse capabilities to monitor Earth's different surfaces (Hansen and Loveland, 2012; Wulder *et al.*, 2012). Others include Microwave Sounding Unite (MSU), Advance Microwave Sounding Unite (AMSU), ASTER SRTM3-DEM, and ALOS are powerful tools for analyzing glacial coverage and/or retreat (Bolch, 2007; Prasad *et al.*, 2011; Liu *et al.*, 2013).

Different research projects that investigated the causes of glacier retreat globally. Snow albedo reduction due to aerosol deposition on snow glaciers is one of the most common topics where remote sensing data are utilized (Lee and Liou, 2012; Prasad *et al.*, 2009; Prasad *et al.*, 2011). Snow has some of the most reflective properties of natural surfaces on Earth (Hadley and Kirchstetter, 2012). It is with these reflective properties that snow and glaciers reflect almost all solar radiation that comes into contact with its surface. However, the addition of dark impurities on snow surfaces decreases its reflectance (known as albedo) and increases its absorption of solar radiation (Hadley and

---

[*] Corresponding author.

E-mail address: elaskary@chapman.edu

Kirchstetter, 2012). Aerosols mix with snow through wet deposition in the snowfall and direct dry deposition on the surfaces (Lee and Liou, 2012). The amount of solar radiation absorbed by the surface could significantly increase through a marginally decrease in snow albedo, thereby further reducing snow albedo (Lee and Liou, 2012). This forms a positive radiative forcing, causing global and regional warming as less solar radiation is reflected back into space (Hadley and Kirchstetter, 2012). This mechanism of snow albedo feedback has been recognized as the most important positive amplification of the global surface temperature warming (Lee and Liou, 2012).

Aerosol particles can heat the atmosphere by absorbing shortwave radiation and releasing longwave radiation, which can change the tropospheric moisture status and stability and further influence the formation of cloud and its existence time through affecting the evaporation process of cloud particles. The presence of absorbing aerosols in the atmosphere reduces the solar radiation that reaches the ground. Meanwhile, the absorbing aerosols heat the atmosphere, thus increasing the vertical stability and affecting the occurrence and development of convection. Some studies have concluded that the net radiation effect of dust aerosols is cooling on the ground and the heating of the aerosol layer (Carlson and Benjamin, 1980). Convective clouds are the main cloud system of precipitation in the earth-atmosphere system and are the main carriers for the exchange of water vapor, trace gases and aerosols in the troposphere. Convective clouds affect the balance of heat in the troposphere through the release of latent heat of water vapor, thus driving the major circulation in the atmosphere (Cui *et al.*, 2006). Convective cloud systems are more sensitive to atmospheric aerosols, which help us to better understand the interactions between aerosols and climate by studying the interaction between cumulus and aerosols (Graf, 2004).

Aerosol deposition from dust storms has become significant events in recent history. Poor management of Earth's dry land has been a concern, such as reducing surface vegetation cover, which increases dust storms from deserts (Al-Saadi *et al.*, 2005). A dust storm can transport large amounts of sand unexpectedly, carrying large amounts of sand, silt, dust, and aerosol particles over long distances that affect different regions, locally and globally (Harrison *et al.*, 2001). The deserts around the Arabian Peninsula and Sahara desert are the main terrestrial sources of sand and dust, with some contributions from Iran, Pakistan and India (Al-Saadi *et al.*, 2005). In the regions of Asia, the main dust source is the Gobi Desert, which affects the Central Asia and Eastern Asia sand events, especially affecting the environments in China and Mongolia (Xu *et al.*, 2009). As a consequence, China's significant dust storms deposit dust into the Pacific, and even influence the environments in western America (Hadley *et al.*, 2007).

Dust aerosols, on the one hand, change the radiation balance of the earth-atmosphere system by absorption and scattering of solar radiation, on the other hand, as cloud condensation nuclei (CCN) and atmospheric ice nuclei (IN), alter the cloud microphysics and precipitation processes.

Because of the wide spectrum of mineral dust distribution, the incident visible radiation and outgoing longwave radiation can be scattered at the same time. Compared with sulfate aerosol, dust particles have larger size and optical thickness, and stronger absorption of solar shortwave radiation. Dust aerosols, when transported from the source to downstream areas, could combine with natural sources such as sea salt particles or sources of pollution such as black carbon, sulphate and nitrate aerosols, thus changing their physical-chemical properties.

Recent studies have shown that dust aerosol has an important contribution to the formation of ice clouds and the transition of vapor phase in clouds. Dust aerosols might impact glacier climate directly by altering the absorbing and scattering rate of the solar and earth radiation (Charlson *et al.*, 1992; Aoki *et al.*, 2005; Hayasaka *et al.*, 2006; Wang *et al.*, 2010; Liu *et al.*, 2011). Sakai *et al.* (2004) analyzed the observation data of a sand-dust weather process and showed that rich mineral aerosol in dust layer provided a large amount of IN for the ice crystal formation process, evenly mixture of ice crystal cloud and sand in the dust layer. Observations by Demott *et al.* (2003) also showed that dust in Asia can be used as an effective IN to increase the concentration of ice crystals in the cloud. Studies by Sassen *et al.* (2002) showed that the air masses originating from sub-Saharan, at lower supersaturations, could freeze in –5°C to –9°C, which fully demonstrated that dust aerosols could be used as effective IN for the cloud process. Kelly *et al.* (2007) analyzed the activation of dust particles of different sizes and concluded that the activation of different dust particles is related to their particle size. For instance dust particles with size less than 0.6 μm, unless wrapped with highly soluble substances, will not become CCN. While dust particles larger than 2 μm in diameter are activated regardless of their composition. It is noteworthy that adhesion of a small amount of soluble substances can increase solubility of the dust particles between 0.6–2 μm. Trochkine *et al.* (2003) analyzed the ACE-Asia data and concluded that changes occurred to the chemical composition of mineral aerosol during the long-distance transportation from China to Japan, thus increasing the soluble components of dust particles and increasing their chances of becoming CCN.

STUDY AREA

The Sierra Nevada mountain range is the largest in California, extending 400-miles north–south and 50-miles east–west, with a coverage of 24,370 square miles. The mountains began to form 200 million years ago, from the formation of granitic rocks. The climate in the Sierra Nevada is Mediterranean with wet, cool winters and dry, long summers (Soulard, 2012). The main source of fresh water supplied to the state of California comes from the Sierra Nevada, with the snowmelt providing an average of 15 million acre-foot of water per year (Sierra Nevada Conservancy, 2011). Each year, 60% of California's total annual precipitation falls on the Sierra Nevada mountain range as rain or snow, which is about 10–90 inches of rain

(Lauer, 2011). The rainfall and snowmelt from the Sierra Nevada travel hundreds of miles along the Sacramento-San Joaquin Delta, with 50% of water flow into the Delta originating from the Sierra Nevada (Sierra Nevada Conservancy, 2011). This study focuses on an area of the Sierra Nevada region shown in Fig. 1.

RETREAT OF THE SIERRA NEVADA GLACIERS

Data

Six imageries obtained from Landsat 5 TM, Landsat 7 ETM+, and Landsat 8 OLI at 30-meters spatial resolution were utilized in this study over a 17-year period, shown in Fig. 2. The scenes chosen for this study were April 6, 2000 (cloud free), from Landsat 7 ETM+; April 20, 2008 (4% cloud coverage), from Landsat 5 TM; April 26, 2016 (6% cloud coverage), from Landsat 8 OLI; August 20, 2000 (cloud free), from Landsat 5 TM; August 26, 2008 (cloud free), from Landsat 5 TM; and August 16, 2016 (0.7% cloud coverage), from Landsat 8 OLI. All of these scenes were collected from path row/number 42/34 and they were projected to UTM 11 zone with reference datum WGS 84. Band 2 (0.52–0.60 μm) and Band 5 (1.55–1.75 μm) were used for Landsat 5 and 7 because that is where the information regarding snow and glaciers is contained. Band 3 (0.53–0.59 μm) and Band 6 (1.57–1.65 μm) were used for Landsat 8 scenes for the same reason.

Identification of Snow Cover

The purpose of this research work is to investigate the recent glacier retreat of the Sierra Nevada Mountains in California from 2000–2016, and identify the causes that are attributed to this glacial retreat. The research aims to use Landsat imagery to examine the changes of glacier retreat of a chosen region in the Sierra Nevada mountain range during winter of April 2000/2016 and summer of August 2000/2016. The study period is selected based on the fact that April is typically the time that Sierra snowpack reaches its peak after series of winter storms, while August is the end of the ablation period. Such selection allows the identification of snow cover at its possible maximum and minimum levels. We compare the changes of snow content of the same month for different years, and see the changes to glacier amount in this region. Many image processing techniques has been applied here as represented in Fig. 3, which summarizes the logical flow and sequence of the image processing steps applied here.

ISODATA classification method was performed on six subset images to distinguish the water class from the other classes. Non-water masks were created based on the classification results and applied on the images. After the water was masked out from the images, Normalized Difference Snow Index (NDSI) was adopted to derive the snow coverage in the study region. A number of studies have shown that NDSI is an effective index for separating snow from other similar features, such as soil, rock and vegetation, and to successfully delineate the glacier cover over large areas (Dozier, 1989; Hall *et al.*, 1995; Sidjak and Wheate, 1999; Racoviteanu *et al.*, 2009; Gardelle *et al.*, 2013). The NDSI was developed based on the fact that snow presents a strong difference in reflecting the visible wavelength and middle infrared wavelengths (Hall *et al.*, 1995). For Landsat 5 and 7 imageries, the index is defined as:

$$NDSI = \frac{Band\,2 - Band\,5}{Band\,2 + Band\,5} \tag{1}$$

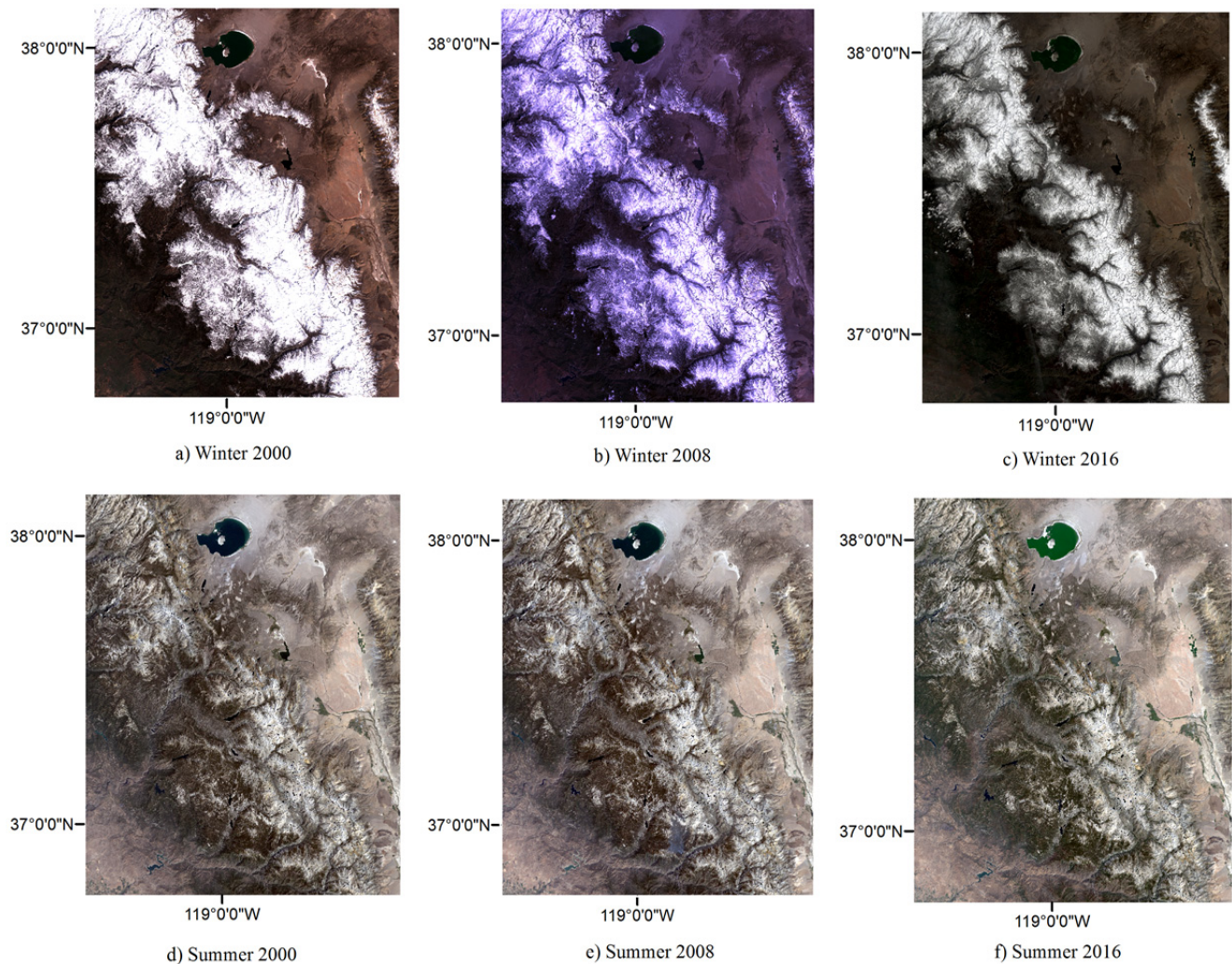**Fig. 1.** Base map showing the target area being studied.

Fig. 2. a), b), and c) Winter season true color composite of Landsat 7 ETM+ image obtained on Apr. 6, 2000, Landsat 5 TM image obtained on Apr. 20, 2008, and Landsat 8 OLI image obtained on Apr. 26, 2016, respectively. d), e), and f) Summer season true color composite of Landsat 5 TM image obtained on Aug. 20, 2000, Landsat 5 TM image obtained on Aug. 26, 2008, and Landsat 8 OLI image obtained on Aug. 16, 2016, respectively.

Also, for Landsat 8 imageries, the index is defined as:

$$NDSI = \frac{Band\,3 - Band\,6}{Band\,3 + Band\,6} \qquad (2)$$

NDSI thresholds need to be determined to identify the snow feature. It is suggested that no fixed threshold values are existed (Hall *et al.*, 1995). They can be chosen manually based on the characteristics of the scenes, such as topography, sun position and haze (Racoviteanu *et al.*, 2008a, b). Also, they can be estimated through the visual inspection of the scenes (Dozier, 1989). For instance, Racoviteanu *et al.* (2008b) identified the snow/ice cover with the NSDI greater than a threshold of 0.7 for the Sikkim Himalaya, India, while Racoviteanu *et al.* (2008a) selected a threshold range of 0.5–0.6 to distinguish the snow feature for the Cordillera Blanca, Peru. For this project, based on the considerations of both characteristics and visual inspection of the scenes, a threshold value of 0.7 was selected and
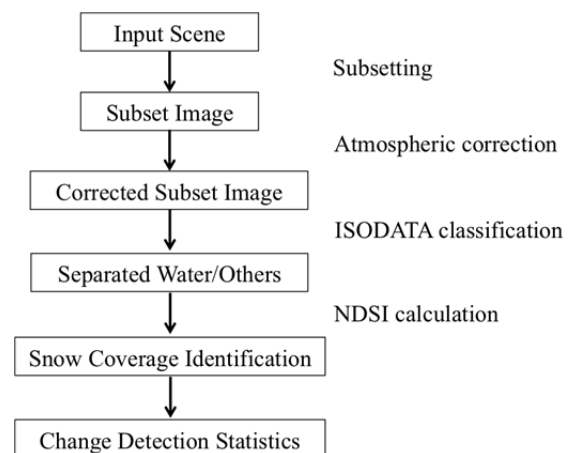

Fig. 3. Steps of image processing.

applied on the 2000 images and a threshold value of 0.6 was selected and applied on 2008 and 2016 images. The

snow coverage was identified for six images using NSDI and is shown in Fig. 4. As seen in Fig. 4, for both winter and summer seasons, the snow cover in the year of 2016 shows much less coverage than that in the year of 2008 and 2000. Such visual inspection indicates a possible retreat in the amount of glacial snow packs over the 17-year period.

Analysis of Snow Cover Change

A common technique known as change detection analysis is employed to quantify the differences among the imageries of the same scene over different dates (El-Askary *et al.*, 2014). The change detection statistics helps quantify the exact amount of glacier retreat for each scene. Such analysis was executed to determine the changes of snow cover between the year of 2000 and 2016 for winter and summer seasons. For the winter season, the snow cover derived from April 2000 scene was used as the initial state and snow cover derived from April 2016 scene was used as the final state. A change detection difference map was generated to show the changes of the snow cover spatially. Meanwhile, the change detection statistics were summarized to quantify the changes. The same procedures were repeated for the summer season. The results are displayed in Fig. 5 and Table 1. As seen in the Fig. 5, there is a significant decrease of snow cover for winter season over the 17-year period, despite a few increasing spots. This is confirmed by data presented in Table 1 that the winter season has a decreasing trend of snow cover based on the snow pixel counts from 2000 to 2008 and further to 2016. The change percentage reveals an overall 76.4% reduction in snow cover from April 2000 to April 2016 over the study area. For the summer season, almost all of the snow cover decreased from August 2000 to August 2016 as shown in Fig. 5. Such declining tendency is also observed from snow pixel counts in Table 1. The correspondent change percentage reaches a high reduction rate of 91.4% in the study region. These results indicate that the Sierra Nevada glaciers experienced a retreat of the snow cover from the year of 2000 to 2016 for both winter and summer seasons in the study area. It is noteworthy that the change map Fig. 5(b) resulting from the changes between the initial map of 2000 summer snow and the final map of 2016 summer snow
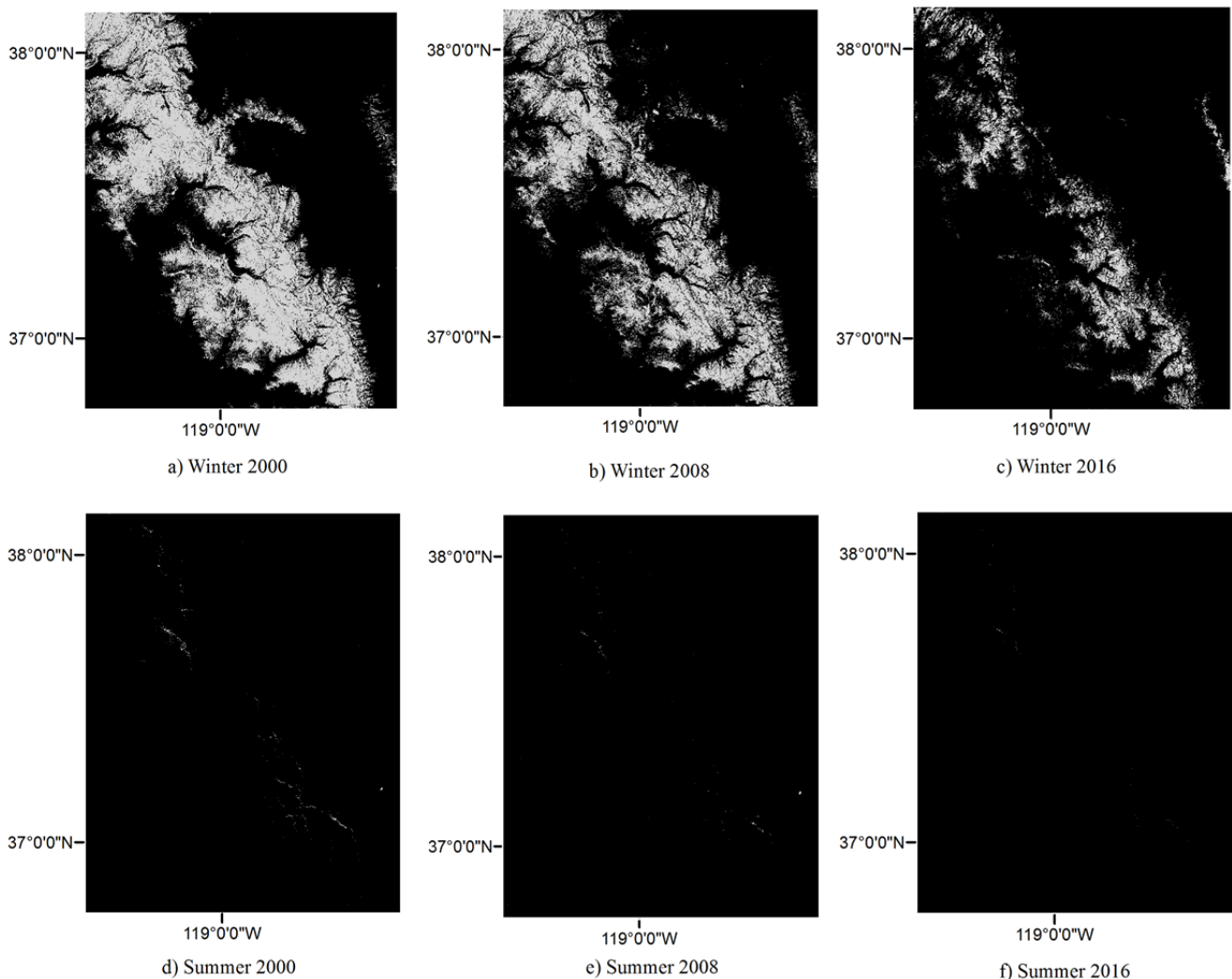

a) Winter 2000   b) Winter 2008   c) Winter 2016

d) Summer 2000   e) Summer 2008   f) Summer 2016

Fig. 4. Winter and Summer seasons snow cover derived from Landsat imageries during April and Augsut of (a, d) 2000, (b, e) 2008 and (c, f) 2016, respectively. The white area denotes the snow cover and black area denotes other land covers.
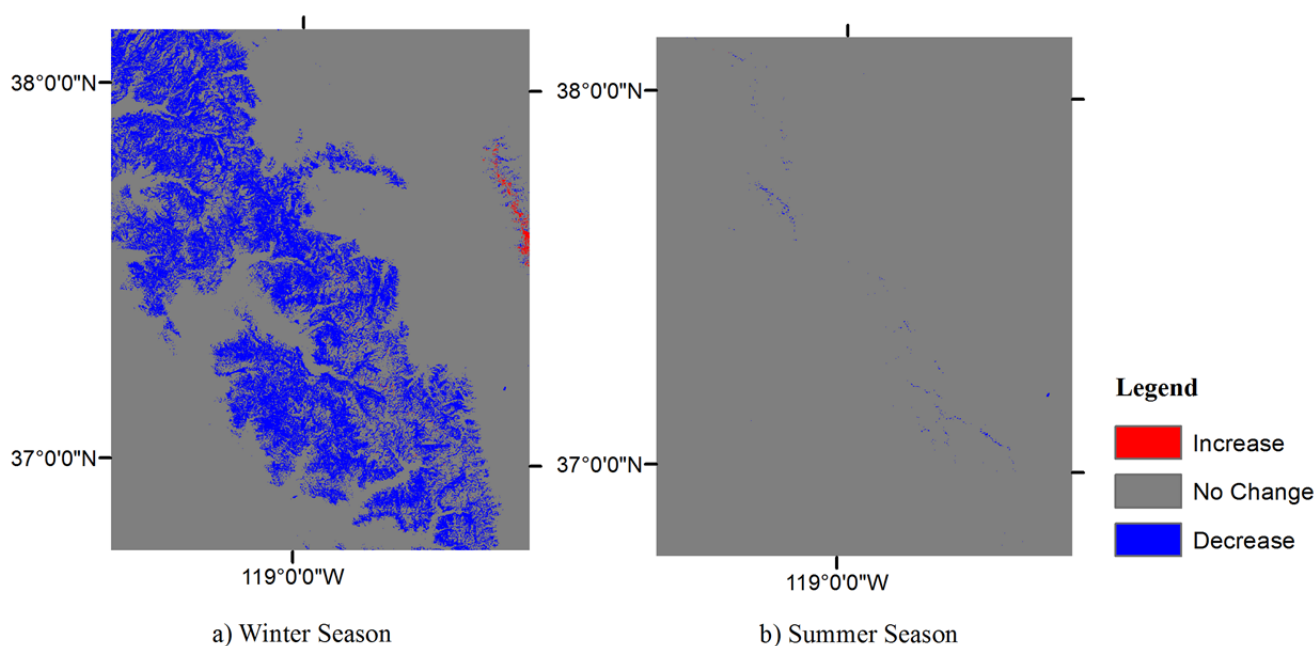
a) Winter Season   b) Summer Season

Fig. 5. Change detection difference maps between 2000 and 2016 for a) winter season and b) summer season, respectively. The grey area represents no change, red area represents the increased snow cover, and blue area represents the decreased snow cover.

Table 1. Change detection statistics of winter and summer season.

Season	Year	Snow pixel counts	Change percentage
Winter	2000	6247127	76.4% of decrease between 2000 and 2016
	2008	4430476	
	2016	1476297	
Summer	2000	18412	91.4% of decrease between 2000 and 2016
	2008	4856	
	2016	1582	

don't show much change as noted by the blue color. This is due to the fact that not much snow was even detected in initial map of 2000. Therefore, most of the 2000 summer snow has disappeared when compared to the 2016 summer snow represented by the blue color.

AEROSOL IMPACT ON SIERRA NEVADA RETREAT

Data

In order to assess the role of aerosol-related impact in the Sierra Nevada glaciers, we used the NASA Goddard Online Interactive Visualization ANd aNalysis Infrastructure (GIOVANNI) tool to obtain and process the data from the Modern-Era Retrospective analysis for Research and Applications version 2 (MERRA-2) and North American Land Data Assimilation System (NLDAS) within the region of (118.5°W, 37°N, 119.5°W, 38°N).

MERRA-2 is a NASA atmospheric reanalysis dataset based on historical climate analysis using the Goddard Earth Observing System Model, Version 5 (GEOS-5), with its Atmospheric Data Assimilation System (ADAS), version 5.12.4. In this research the MERRA-2 data includes Snow

Depth, Surface Air Temperature, Snowfall on Land, Surface Albedo for Near Infrared Diffuse, Surface Albedo for Visible Diffuse, as well as Total Aerosol Extinction AOD at 550 nm. All the MERRA-2 data used is at $0.5° \times 0.625°$ resolution with monthly or hourly time scales over January 2000 to December 2016.

The NLDAS is a collaboration project among several groups: NOAA/NCEP's Environmental Modeling Center (EMC), NASA's Goddard Space Flight Center (GSFC), Princeton University, the University of Washington, the NOAA/NWS Office of Hydrological Development (OHD), and the NOAA/NCEP Climate Prediction Center (CPC). The goal of the project is to improve the results of numerical weather prediction models through providing quality-controlled, and spatially and temporally consistent, land-surface model (LSM) datasets from the best available observations and model output. Extended back to January 1979, NLDAS provides near real-time data with a 0.125° resolution and hourly to monthly time scales over central North America. In this research we analyzed the NLDAS Mosaic (MOS) Noah datasets including Anomaly of Snowfall (frozen precipitation) (data of February and March 2016 are missing), Anomaly of Snow Cover Fraction (data

of February and March 2016 are missing), Surface Incident Longwave Radiation Flux and Surface Skin Temperature over January 2000 to December 2016.

Moreover, we analyzed related parameters from AERONET (AErosol RObotic NETwork) station at Fresno, including the Angstrom Parameter, Spectral De-Convolution Algorithm (SDA) aerosol optical depth retrievals, and GSFC (Goddard Space Flight Center) Back-trajectory analysis to study a high aerosol event during April 18–19 of 2004. Established by NASA and PHOTONS (PHOtométrie pour le Traitement Opérationnel de Normalisation Satellitaire; Univ. of Lille 1, CNES, and CNRS-INSU), as well as collaborators from institutes, universities and other partners, the AERONET project is a worldwide ground-based remote sensing aerosol networks. AERONET has provides long-term, continuous and accessible database of aerosol optical, microphysical and radiative properties for aerosol research over 25 years. In this study, we used the observation data at Fresno (119.773167°W, 36.781733°N), which is the closest available AERONET station near Sierra Nevada glaciers. Angstrom Parameter could estimate the size distribution of aerosols from spectral aerosol optical depth (AOD). The negative slope (or first derivative) of AOD with wavelength in logarithmic scale is known as the Angstrom parameter (α), which could be calculated from two or more wavelengths using a least squares fit. Values of α greater than 2.0 indicate fine mode particles such as smoke particles and sulfates, while values of α near zero indicate the presence of coarse mode particles (e.g., desert dust). Retrievals of AOD with SDA algorithm yields fine (sub-micron) and coarse (super-micron) aerosol optical depths at a standard wavelength of 500 nm, where the fraction of fine mode to total aerosol optical depth can be computed. This algorithm produces useful indicators of aerosol size discrimination at the frequency of extinction measurements. Generated as twice a day (00Z and 12Z), GSFC 7 days Back-trajectory is a kinematic trajectory analysis using NASA GMAO (Global Modeling Assimilation Office) assimilated gridded analysis data and from NCEP (National Centers for Environmental Prediction) analyses.

The Impact of Snowfall and Temperature on Sierra Nevada Retreat

In order to reveal the aerosol and snow interaction in Sierra, we initially attempted to study factors such as snowfall and surface air temperature, which directly influence the snow coverage. From Fig. 6(a), a strong correlation (0.599) between the variations of snowfall and snow cover anomalies is evident. This suggests that snowfall is the critical contributing factor to the snow coverage in this area. In Fig. 6(b), snow depth during middle summer (July and August) equals to 0, meaning that snow cover in this region is mostly composed of winter and spring snowfall, which supports the previous result that the snowfall dominating the snow coverage in Sierra Nevada. It is logical that higher temperature accelerates the melting process of snow, which could be seen in the negative relationship (–0.265) between surface air temperature anomaly and snow depth. It is clearly shown that the pattern of "high snowfall & high snow cover, low temperature & high snow depth" during the period of 2010 to 2011, as well as "low snowfall & low snow cover, high temperature & low snow depth" during the period of 2012 to 2015. In this paper, we will approach the impact of
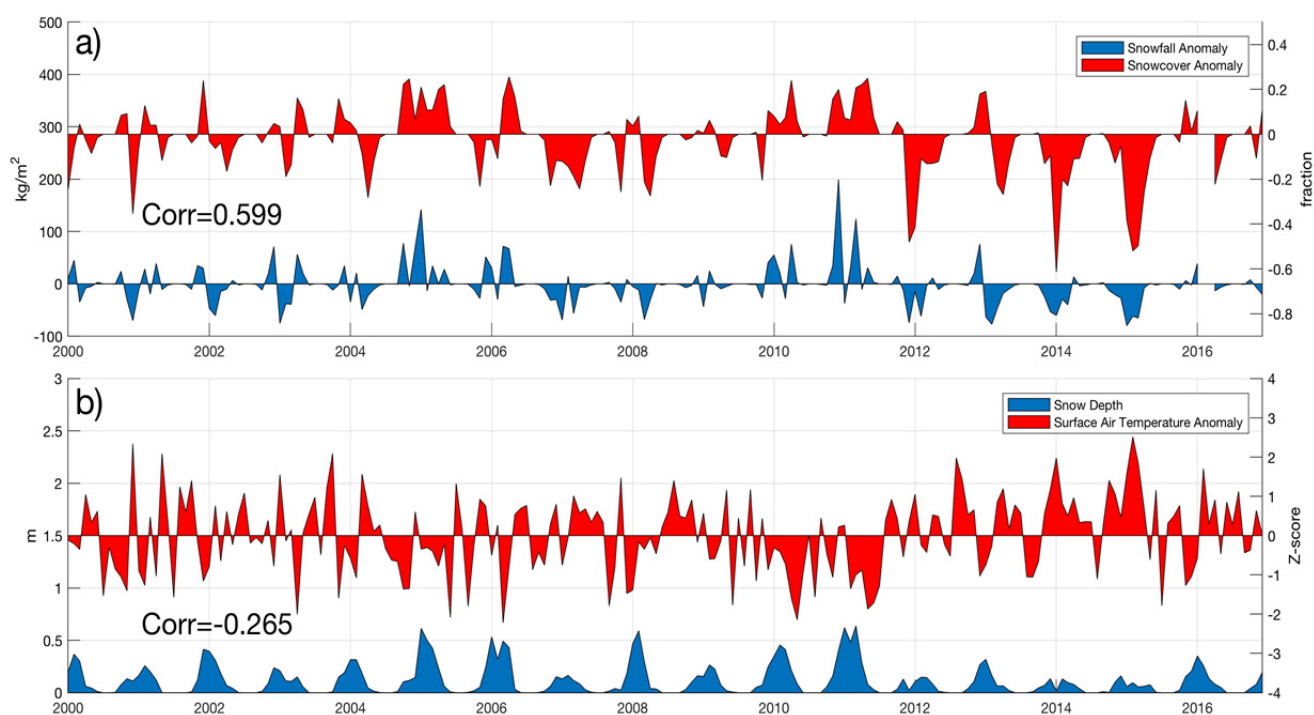

Fig. 6. The variation of (a) Snowfall anomaly and snow cover anomaly; (b) Snow depth and surface air temperature anomaly; as well as parameter correlation coefficients in (a) and (b).

aerosols on snow coverage in this area by studying aerosols and the effect on the snowfall and temperature.

Correlation Analysis of AOD and Snowfall Anomalies

In Fig. 7, from the analysis of intra-annual AOD variations we conclude that the AOD values stay high during the period from March to August, and low during September to February. The plots of less snow period (September–November) and major snowfall period (December–February) show a negative relationship between AOD and snowfall anomalies (correlation of September = –0.193, October = –0.052, November = –0.332, December = –0.379, January = –0.078, February = –0.205). We recognize the low correlation coefficient values, yet the negative behavior implies on the process of the snowfall that enhances aerosols absorption. On the other hand, during the spring and summer period (March–August), it shows a weak positive relationship between AOD and snowfall anomalies (correlation of March = 0.122, April = 0.060), which indicates the high aerosol activity may improve the process of snowfall formation/precipitation. It also shows a negative relationship (correlation of May = –0.186, June = –0.241) or no relationship (July and August due to no snowfall record). It is clear that only one anomalously high snowfall event was recorded during June of 2011 and not during any other Junes. Therefore, it is evident that the period from June to August, according to the snowfall records, is not relevant to our analysis here due to the limited, if any, snowfall during these months. In general, the analysis of AOD and snowfall variations implies a negative relationship. It is noteworthy that the sources and types of aerosols during

the year might not be alike. Different types of aerosols, regardless their intensities, could exert different influences on the snowfall precipitation.

Analysis of AOD and Snowfall of April

To further investigate the relation between dust outbreaks and their possible impact on snowfall during the winter season, a detailed analysis is carried out on the hourly scale for both AOD extinction and snowfall during the month of April for the years from 2000 to 2016. Fig. 8 shows the snowfall values during April for each year as a histogram. It is clear that most snowfall events are small ($\leq$ 2 kg m^{-2}), with highest record (> 6 kg m^{-2}) on April 7, 2001, and almost no snow recorded during April 2008. The AOD values mostly remains low (< 0.2) during April of 2000 to 2016, with several high records (≥ 0.4) during the years of 2001, 2004, 2005, 2006 and 2015, among which April 19, 2004, reaches almost 0.6 as the highest value of AOD recorded. A snow event is also recorded on the same day causing a subsequent drop in the AOD values the following day because of possible deposition. This behavior could provide a helpful insight on the aerosol and snow interactions. In general, during the month of April over all the presented years, when a high AOD loading is observed, matching a snowfall event, a drop in the AOD value is observed on the following days.

Study of the AOD Event during April 15–20 of 2004

From Fig. 9(a), the albedo diffusion of both NIR and visible bands increased after snowfall started around April 17, then decreased right after the occurrence of the AOD
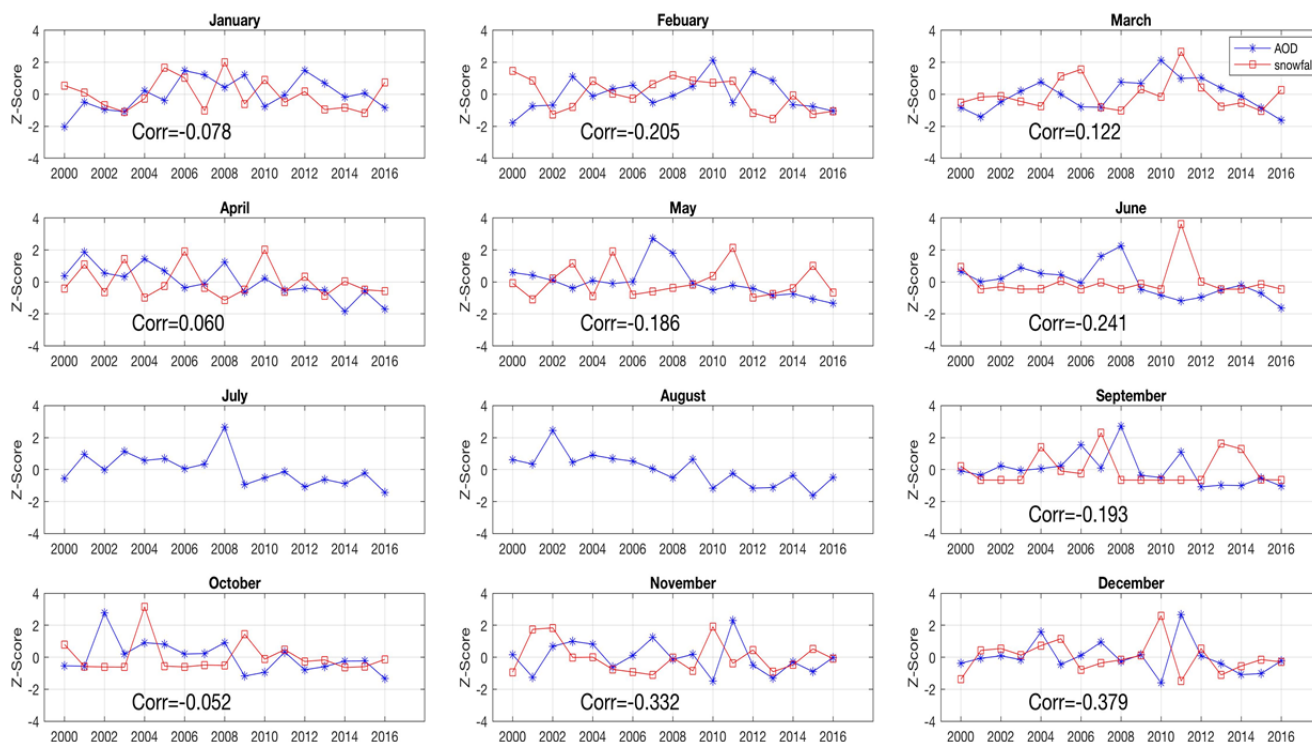

Fig. 7. Z-score for each month as variations of AOD and snowfall anomalies, as well as correlation coefficient in each month during 2000 to 2016.
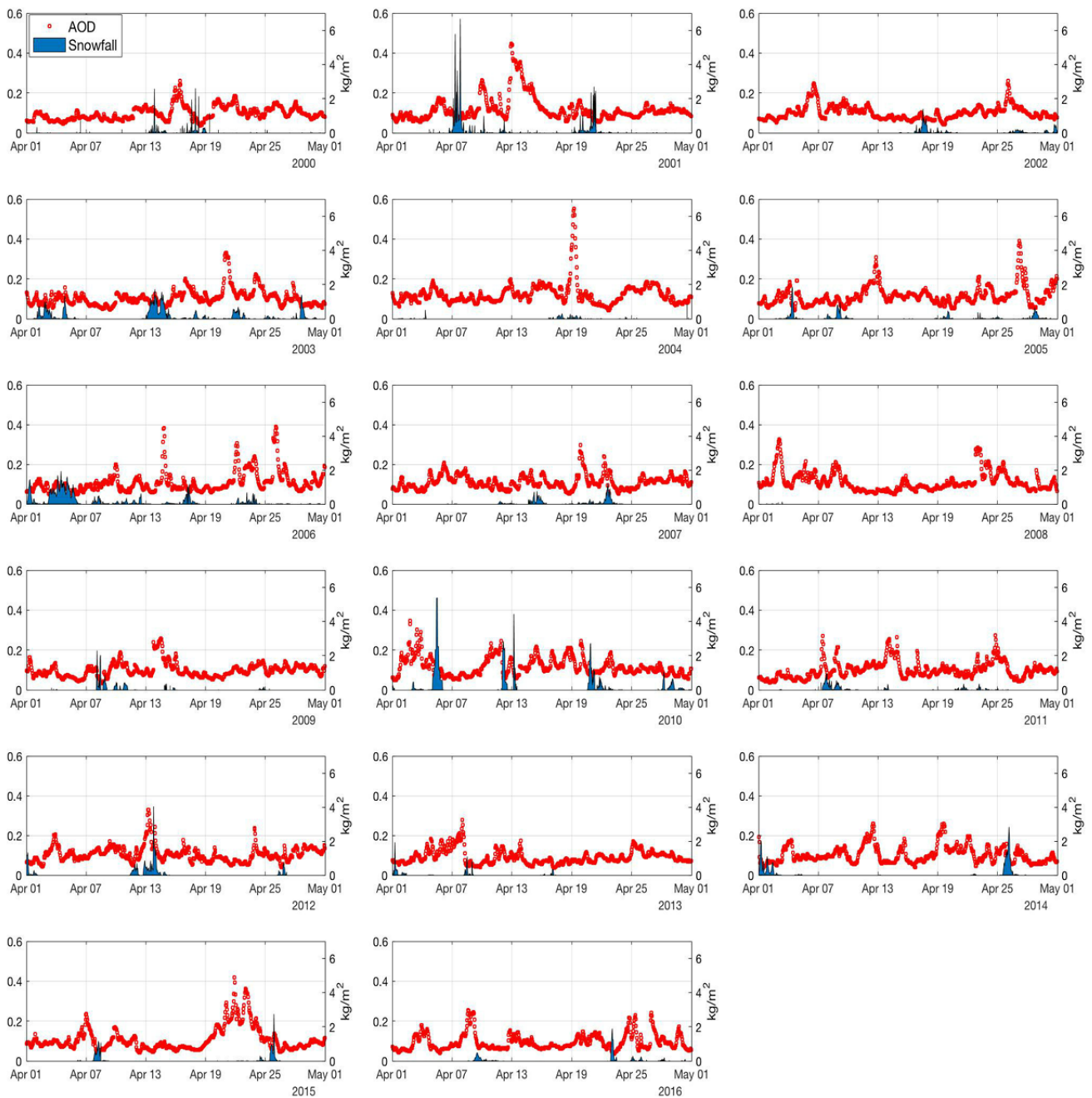
Fig. 8. Hourly AOD and snowfall during April for each year during 2000 to 2016.

event at the afternoon of April 18. Albedo values peaked during the afternoon of April 19, then kept on decreasing after the snowfall ended on April 20. The sudden drop of the albedo values right after the AOD event indicates the deposition of aerosols that might cover the snow surface and hence contributes in decreasing the albedo values. Fig. 9(b) shows the increase in values of both absorbed and incident longwave radiation, yet the absorbed is still higher than the increase of incident longwave radiation flux, confirming the decrease in the albedo values, since the surface absorbed more energy during aerosols' deposition conditions than the non-aerosol affected conditions. Both NLDAS MOS and NOAH models show a decreasing trend

of surface skin temperature, while after the start of AOD event the values of the lower temperature for both models even simulated higher than the values before the snowfall as shown in Fig. 9(c). This abrupt change supports what is found in Fig. 9(b). The physical background for interpreting the effects of radiation flux on the snowpack melt, associated with aerosols deposition, is based on the increase of the absorbed energy that raised the average snowpack temperature leading to more melt.

In summary the deposited aerosols affected the albedo of snow surface to change the heat flux, increase the surface temperature, and then accelerate the melting process of snow cover. However, different kinds of aerosol deposition
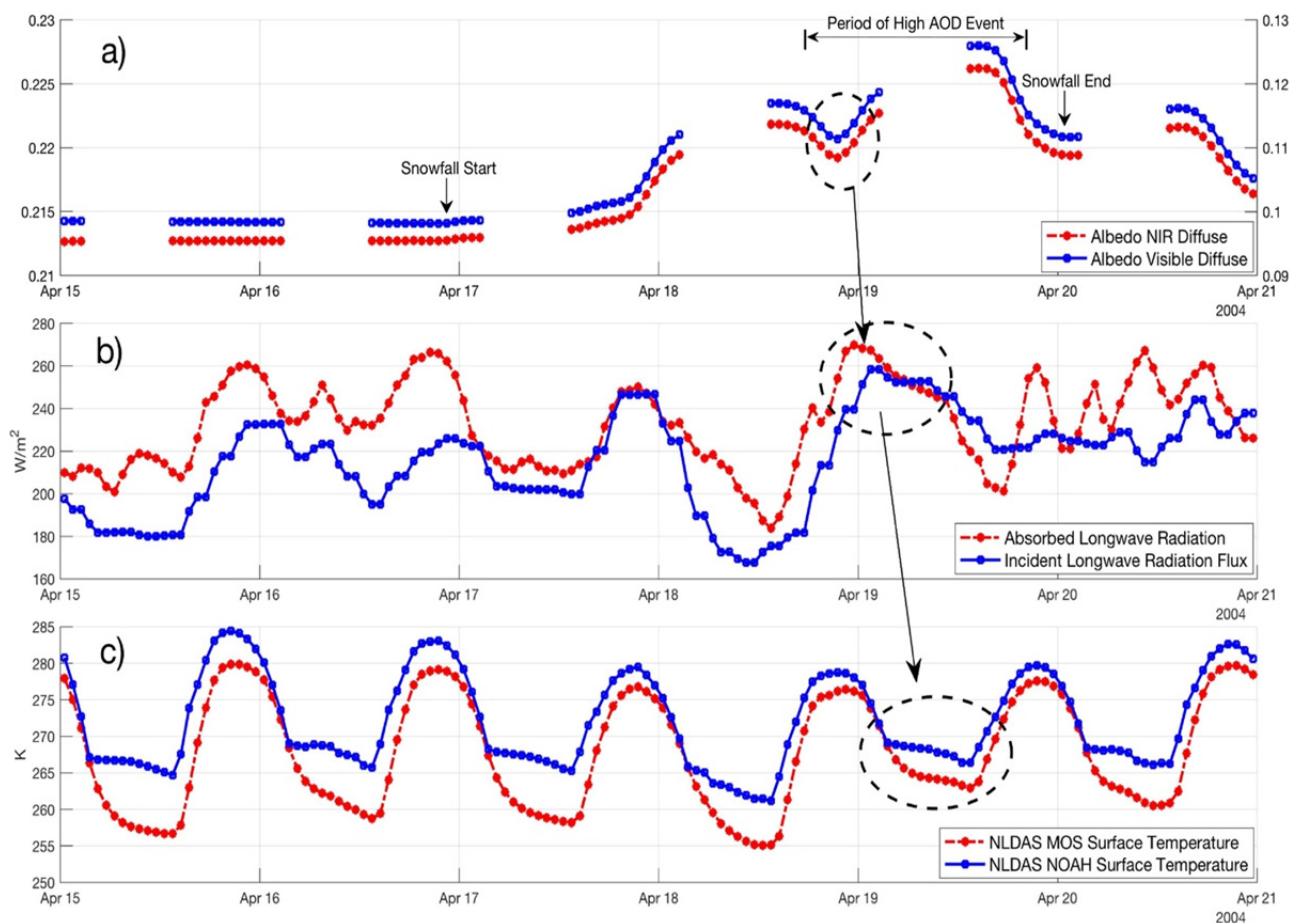
Fig. 9. (a) Albedo NIR/Visible diffuse; (b) Surface absorbed longwave radiation/surface incident longwave radiation flux; (c) NLDAS MOS/NOAH surface temperature data during the period of April 15–20 of 2004.

affect the melting process in distinct ways. The black carbon could function more effectively than other kinds such as sea salt or dust deposition. In order to explore the sources of the aerosols of this AOD event, we collected AOD data from the morning of April 15 to midnight of April 19, to track the entire life cycle of generation of the AOD event.

The left side of each panel in Fig. 10 shows the aerosols transportation from eastern Asia, dust (mostly from northern China) and pollution (from both northern and southern cities of China) assembled together, moving over Japan then dispersed into the northern Pacific Ocean. Over time as shown in Fig. 10(g) (circled area), aerosols are observed over the Sierra which is confirmed by the low Angstrom exponent measurements obtained from the Fresno AERONET station, SDA retrievals showing fine and coarse mode fractions and the GSFC back trajectory as shown in Figs. 11(a)–11(c). It is evident that the dust originated from those events is moving southeastward over the Pacific Ocean shown in Figs. 10(a)–11(f). From all the above, it is reasonable to suggest that aerosols from eastern Asia are contributing to the aerosols' depositing over the Sierra. These aerosols also passed over the cities along the California coast adding more pollutants from these regions which should also be considered. In summary, we can claim that the aerosols affecting the Sierra area are representing a

mixing scenario between pollutants from both US and Asia cities with the dust from northern Asia as well as the sea salt from the ocean surface, through the processes of the atmospheric circulation and air-sea interactions. These mixing scenarios will be further investigated through a different research manuscript.

CONCLUSION

Because aerosols change the energy balance, and the size and duration of cloud droplets in the earth–atmosphere system, they have a profound impact on the global climate, water cycle, and ecosystem. The absorption and scattering of atmospheric aerosols cause the radiation balance to change, which in turn affects the general circulation of the atmosphere. Additionally, aerosols can participate in microphysical cloud processes, such as the formation of cloud condensation nuclei (CCN) or ice nuclei (IN), which affect the cloud type, life cycle, and cover, resulting in changes in rainfall, such as the intensity and distribution of precipitation. The study presented here contributes to a better understanding of the physico-chemical properties of aerosols and aerosol-precipitation. We first used change detection analysis to identify changes in the winter and summer snowpack from 2000 till 2017. Based on the remote
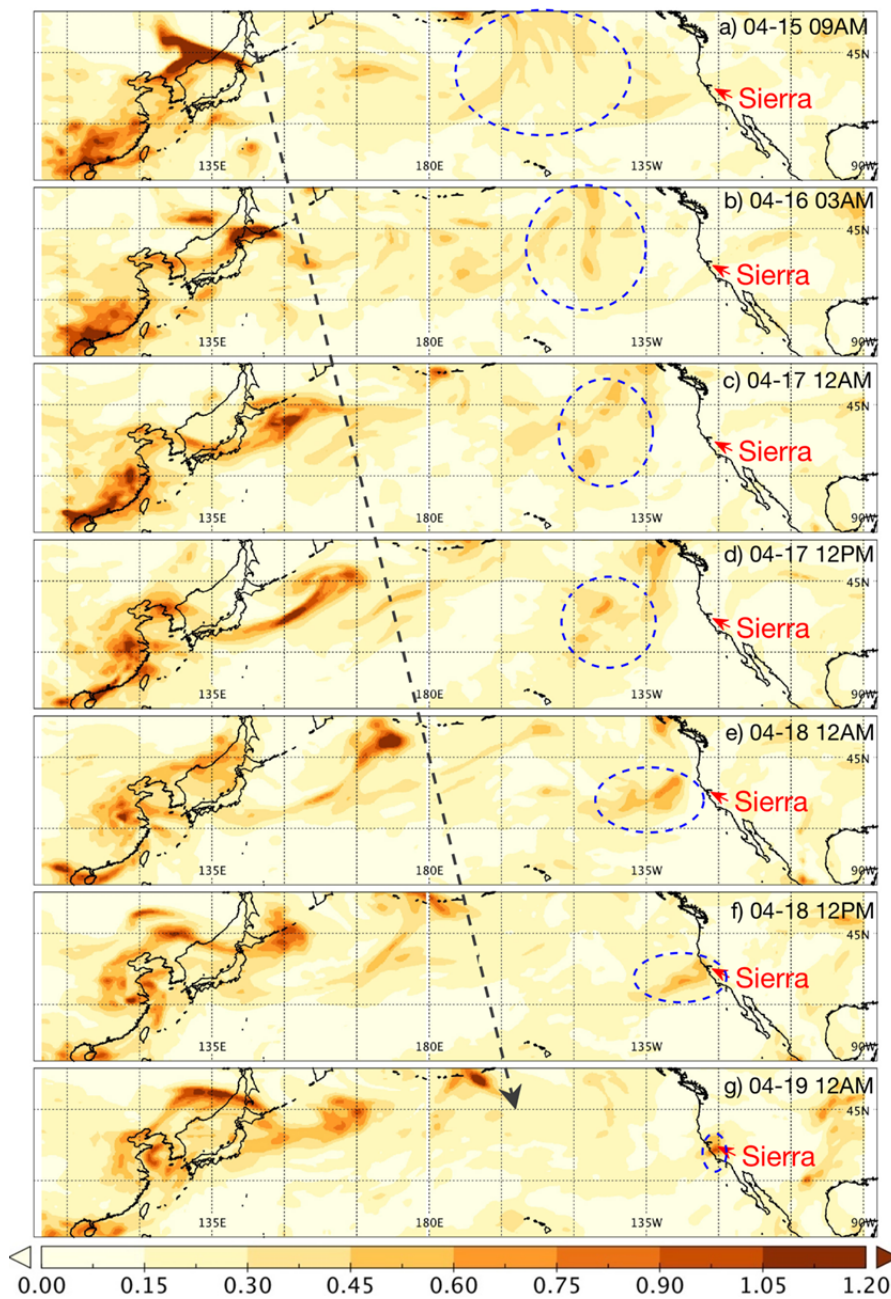
Fig. 10. Aerosol AOD cross the Pacific Ocean during April 14–19 of 2004.

sensing image analysis of LANDSAT in 2000, 2008, and 2016, we found a 76.4% decrease during winter (April) and a 91.4% decrease during summer between 2000 and 2016. These results are in good agreement with the NLDAS model and are more accurate than the model output (which has no value recorded) for changes in the snow cover during summer. Moreover, the results of the MERRA-2 and NLDAS models confirm that snowfall and temperature anomalies are the major factors affecting snow cover in this area. Statistical analysis of the AOD and snowfall anomalies showed a generally negative correlation during all seasons, indicating that aerosols are absorbed by the snowfall. The positive correlation between March and April also implies that aerosols may contribute to increased

snowfall. However, the mechanism of interaction between aerosols and precipitation is rather complicated, and there are many factors affecting the occurrence of precipitation, such as the type and the height of clouds as well as the micro-physical characteristics. During the period of April 15–20, 2004, a high AOD event occurred in this region. Analysis showed decreased albedo on the surface of the snow and increased absorption of radiation, thereby increasing the surface temperature and accelerating the snowmelt. Dust and pollution in East Asia, as well as sea salt in the Pacific, and cities along the coast of California, all contributed to this aerosol event, and the analysis of AERONET data indicates that coarse particles were the principle component. This research uses long-term observations from satellite
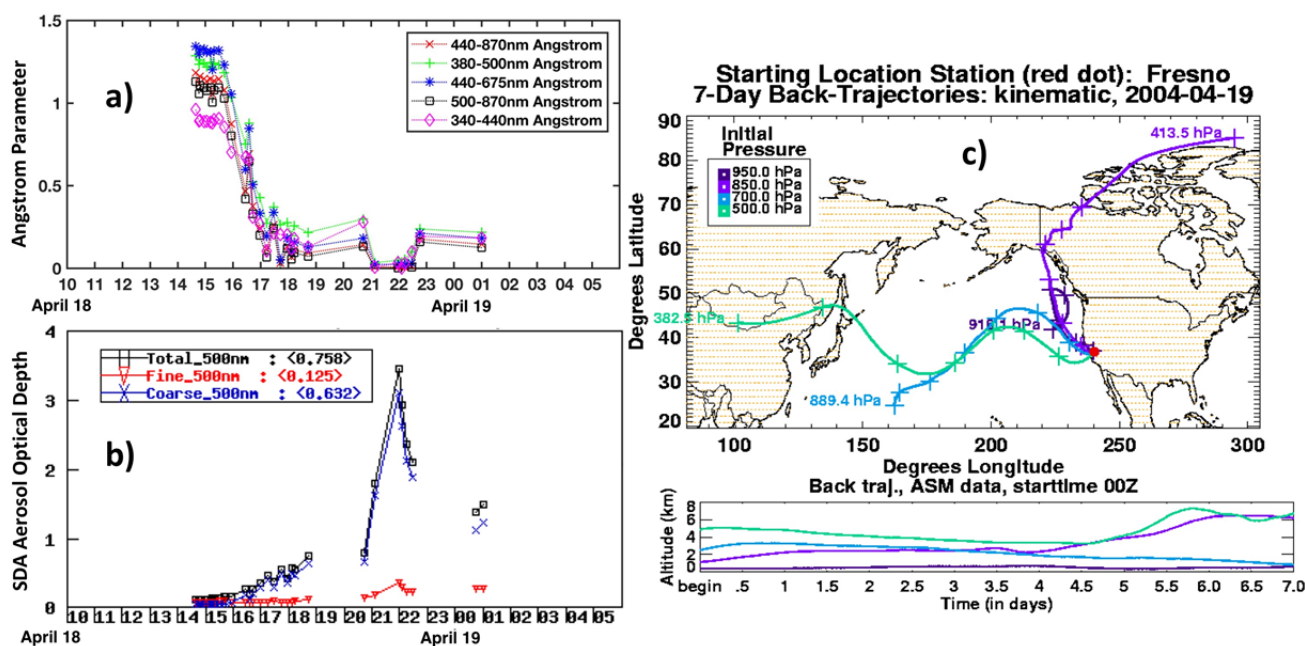
Fig. 11. a) Angstrom Paramter, b) SDA Aerosol Optical Depth, c) Back-Trajectories analysis during April 18–19, 2015.

remote sensing, and numerical simulation data, with emphasis on the statistical relationship between aerosols and snowfall, including a case study of a high aerosol event, to augment knowledge of regional aerosol-snow interaction. It is noteworthy that the reduction of the snowpack is associated with the phase change from a solid to a liquid state. By addressing sensible and/or latent heat fluxes, the physical backgrounds for interpreting the effects of radiation flux on the melting of the snowpack will be investigated in future research.

REFERENCES

Al-Saadi, J., Pierce, R.B., Neil, D., Chu, D.A., Weinstock, L., MacDonald, C. and Wayland, R. (2005). Improving national air quality forecasts with satellite aerosol observations. *Bull. Am. Meteorol. Soc.* 86: 1249–1261.

Bartsch, A., Kumpula, T., Forbes, B.C. and Stammler, F. (2010). Detection of snow surface thawing and refreezing in the Eurasian Arctic using QuikSCAT: Implications for reindeer herding. *Ecol. Appl.* 20: 2346–2358.

Bolch, T. (2007). Climate change and glacier retreat in northern Tien Shan (Kazakhstan/Kyrgyzstan) using remote sensing data. *Global Planet. Change* 56: 1–12.

Carlson, T.N. and Benjamin, S.G. (1980). Radiative heating rates for saharan dust. *J. Atmos. Sci.* 37: 193–213.

Cui, Z., Carslaw, K.S., Yin, Y. and Davies, S. (2006). A numerical study of aerosol effects on the dynamics and microphysics of a deep convective cloud in a continental environment. *J. Geophys. Res.* 111: D05201.

DeMott, P.J., Sassen, K., Poellot, M.R., Baumgardner, D., Rogers, D.C., Brooks, S.D., Prenni, A.J. and Kreidenweis, S.M. (2003). African dust aerosols as atmospheric ice nuclei. *Geophys. Res. Lett.* 30: 1732.

Dozier, J. (1989). Spectral signature of alpine snow cover from the Landsat Thematic Mapper. *Remote Sens. Environ.* 28: 9–22.

El-Askary, H., Abd El-Mawla, S.H., Li, J., El-Hattab, M.M. and El-Raey, M. (2014). Change detection of coral reef habitat using Landsat-5 TM, Landsat 7 ETM+ and Landsat 8 OLI data in the Red Sea (Hurghada, Egypt). *Int. J. Remote Sens.* 35: 2327–2346.

Gardelle, J., Berthier, E., Arnaud, Y. and Kääb, A. (2013). Region-wide glacier mass balances over the Pamir-Karakoram-Himalaya during 1999–2011. *Cryosphere* 7: 1263–1286.

Graf, H.F. (2004). The complex interaction of aerosols and clouds. *Science* 303: 1309–1311.

Hadley, O.L., Corrigan, C.E., Kirchstetter, T.W., Cliff, S.S. and Ramanathan, V. (2010). Measured black carbon deposition on the Sierra Nevada snow pack and implication for snow pack retreat. *Atmos. Chem. Phys.* 10: 7505–7513.

Hadley, O.L., Ramanathan, V., Carmichael, G.R., Tang, Y., Corrigan C.E., Roberts, G.C. and Mauger, G.S.

(2007). Trans-Pacific transport of black carbon and fine aerosols (D<2.5 um) into North America. *J. Geophys. Res.* 112. D05309.

Hadley, O.L. and Kirchstetter, T.W. (2012). Black-carbon reduction of snow albedo. *Nat. Clim. Change* 2: 437–440.

Hall, D.K., Riggs, G.A. and Salomonson, V.V. (1995). Development of methods for mapping global snow cover using Moderate Resolution Imaging Spectroradiometer data. *Remote Sens. Environ.* 54: 127–140.

Hansen, M.C. and Loveland, T.R. (2012). A review of large area monitoring of land cover change using Landsat data. *Remote Sens. Environ.* 122: 66–74.

Harrison, S.P., Kohfeld, K.E., Roelandt, C., Claquin, T. (2001). The role of dust in climate changes today, at the last glacial maximum and in the future. *Earth Sci. Rev.* 54: 43–80.

Hunsaker, C.T., Whitaker, T.W. and Bales, R.C. (2012). Snowmelt runoff and water yield along elevation and temperature gradients in California's Southern Sierra Nevada. *J. Am. Water Resour. Assoc.* 48: 667–678.

Irion, R. (2001). The melting snows of Kilimanjaro. *Science* 291: 1690–1691.

Jepsen, S.M., Molotch, N.P., Williams, M.W., Rittger, K.E. and Sickman, J.O. (2012). Interannual variability of snowmelt in the Sierra Nevada and Rocky Mountains, United States: Examples from two alpine watersheds. *Water Resour. Res.* 48: W02529.

Kapnick, S. and Hall, A. (2008). Observed climate-snowpack relationships in California and their implications for the future. *J. Clim.* 23: 3446–3455.

Kapnick, S. and Hall, A. (2009). *Observed changes in the Sierra Nevada snowpack: Potential causes and concerns*. Rep. CEC-500-2009-016-F. Calif. Environ. Prot. Agency, Sacramento.

Kaser, G., Hardy, D.R, Mölg, T., Bradley, R.S. and Hyera, T.M. (2004). Modern glacier retreat on Kilimanjaro as evidence of climate change: observations and facts. *Int. J. Climatol.* 24: 329–339.

Kayetha, V.K., Senthilkumar, J., Prasad, A., Cervone, G. and Singh, R.P. (2007). Effect of dust storm on ocean color and snow parameters. *J. Indian Soc. Remote Sens.* 35: 1.

Kelly, J.T., Chuang, C.C. and Wexler, A.S. (2007). Influence of dust composition on cloud droplet formation. *Atmos. Environ.* 41: 2904–2916.

Knowles, N., Dettinger, M.D. and Cayan, D.R. (2006). Trends in snowfall versus rainfall in the western United States. *J. Clim.* 19: 4545–4559.

Kulkarni, A.V., Bahuguna, I.M., Rathore, B.P., Singh, S.K., Randhawa, S.S., Sood, R.K. and Dhar, Sunil. (2007). Glacial retreat in Himalaya using Indian remote sensing satellite data. *Curr. Sci.* 92: 69–74.

Lee, W.L. and Liou, K.N. (2012). Effect of absorbing aerosols on snow albedo reduction in the Sierra Nevada. *Atmos. Environ.* 55: 425–430.

Liu, T., Kinouchi, T. and Ledezma, F. (2013). Characterization of recent glacier decline in Cordillera Real of LANDSAT, ALOS, and ASTER data. *Remote*

Sens. Environ. 137: 158–172.

Liu, Y., Shi, G. and Xie, Y. (2013). Impact of dust aerosol on glacial-interglacial climate. *Adv. Atmos. Sci.* 30: 1725–1731.

Lohmann, U. (2002). A glaciation indirect aerosol effect caused by soot aerosols. *Geophys. Res. Lett.* 29: 11-1–11-4.

Mahowald, N.M., Muhs, D.R., Levis, S., Rasch, P.J., Yoshioka, M., Zender, C.S. and Luo, C. (2006). Change in atmospheric mineral aerosols in response to climate. *J. Geophys. Res.* 111: D10202.

Martinuzzi, S., Gould, W.A. and Ramos Gonzalez, O.M. (2007). Creating cloud-free landsat ETM+ data sets in tropical landscapes: Cloud and cloud-shadow removal. In *General Technical Report IITF-GTR-32*. United States Department of Agriculture, Forest Service, International Institute of Tropical Forestry.

Miller, R.L. and Tegen, I. (1998). Cliamte response to soil dust aerosols. *J. Clim.* 11: 3247–3267.

Minder, J.R. and Kingsmill, D.E. (2013). Mesoscale Variations of the Atmospheric Snow Line over the Northern Sierra Nevada: Multiyear Statistics, Case Study, and Mechanisms. *J. Atmos. Sci.* 70: 916–938.

Molotch, N.P. and Bales, R.C. (2006). Comparison of ground-based and airborne snow surface albedo parameterizations in an alpine watershed: Impact on snowpack mass balance. *Water Resour. Res.* 42.W05410.

NASA Landsat science, http://landsat.gsfc.nasa.gov/, Last Access: 21 December 2012.

NOAA El Niño research, forecasts and observations, http://www.elnino.noaa.gov/, Last Access: 21 December 2012.

Panek, J., Saah, D., Esperanza, A., Bytnerowicz, A., Fraczek, W. and Cisneros, R. (2013). Ozone distribution in remote ecologically vulnerable terrain of the southern Sierra Nevada, CA. *Environ. Pollut.* 182: 343–356.

Pierce, D.W., Barnett, T.P., Hidalgo, H.G., Das, T., Bonfils, C., Santer, B.D., Bala, G., Dettinger, M.D., Cayan, D.R., Mirin, A., Wood, A.W. and Nozawa, T. Attribution of Declining Western U.S. Snowpack to Human Effects. *J. Clim.* 21: 6425–6444.

Powell, C., Blesius, L., Davis, J. and Schuetzenmeister, F. (2011). Using MODIS snow cover and precipitation data to model water runoff for the Mokelumne River Basin in the Sierra Nevada, California (2000-2009). *Global Planet. Chang* 77: 77–84.

Prasad, A.K., El-Askary, H. and Kafatos, M. (2010). Implications of high altitude desert dust transport form Western Sahara to Nile Delta during biomass burning season. *Environ. Pollut.* 158: 3385–3391.

Prasad, A.K., El-Askary, H.M., Asrar, G.R., Kafatos, M. and Jaswal, A. (2011). Melting of Major Glaciers in Himalayas: Role of Desert Dust and Anthropogenic Aerosols. In *Planet Earth 2011 - Global Warming Challenges and Opportunities for Policy and Practice,* Carayannis, E.G. (Ed.), Intech, pp. 89–122.

Prasad, A.K., Yang, K.H.S., El-Askary, H.M. and Kafatos, M. (2009). Melting of major Glaciers in the western Himalayas: evidence of climatic changes from long term

MSU derived tropospheric temperature trend (1979-2008). *Ann. Geophys.* 27: 4505–4519.

Racoviteanu, A.E., Arnaud, Y., Williams, M.W. and Ordoñez, J. (2008a). Decadal changes in glacier parameters in the Cordillera Blanca, Peru, derived from remote sensing. *J. Glaciol.* 54: 499–510.

Racoviteanu, A.E., Paul, F., Raup, B., Khalsa, S.J.S. and Armstrong, R. (2009). Challenges and recommendations in mapping of glacier parameters from space. Results of the 2008 Global Land Ice Measurements from Space (GLIMS) workshop, Boulder, Colorado, USA. *J. Glaciol.* 50: 53–69.

Racoviteanu, A.E., Williams, M.W. and Barry, R.G. (2008b). Optical remote sensing of glacier characteristics: A review with focus on the Himalaya. *Sensors* 8: 3355–3383.

Raleigh, M.S., Rittger, K., Moore, C.E., Henn, B., Lutz, J.A. and Lundquist, J.D. (2013). Ground-based testing of MODIS fractional snow cover in subalpine meadows and forests of the Sierra Nevada. *Remote Sens. Environ.* 128: 44–57.

Raub, W., Brown, C. S. and Post, A. (2006). *Inventory of Glaciers in the Sierra Nevada, California.* U.S. Geological Survey (USGS), California, Open-File Report 2006-1239, 232 p.

Rittger, K., Kahl, A. and Dozier, J. (2011). Topographic distribution of snow water equivalent in the Sierra Nevada, paper presented at the 2011 Western Snow Conference, Lake Tahoe, Neveda, 18–22 April.

Rittger, K., Painter, T.H. and Dozier, J. (2013). Assessment of methods for mapping snow cover from MODIS. *Adv. Water Resour.* 51: 367–380.

Sakai, T., Nagai, T., Nakazato, M. and Matsumura, T. (2004). Raman lidar measurement of water vapor and ice clouds associated with Asian dust layer over Tsukuba, Japan. *Geophys. Res. Lett.* 31: L06128.

Sassen, K. (2002). Indirect climate forcing over the western us from asian dust storms. *Geophys. Res. Lett.* 29: 103-1–103-4.

Sidjak, R.W. and Wheate, R.D. (1999). Glacier mapping of the Illecillewaet icefield, British Columbia, Canada, using Landsat TM and digital elevation data. *Int. J. Remote Sens.* 20: 273–284.

Solomon, S., Qin, D., Manning, M., Chen, Z., Marquis, M., Averyt, K.B., Tignor, M. and Miller, H.L. (2007). *Climate change 2007: The physical science basis.* Cambridge University Press, Cambridge.

Trochkine, D., Iwasaka, Y., Matsuki, A., Yamada, M., Kim, Y.S., Nagatani, T., Zhang, D., Shi, G.Y. and Shen, Z. (2003). Mineral aerosol particles collected in Dunhuang, China, and their comparison with chemically modified particles collected over Japan. *J. Geophys. Res.* 108: 8642.

VanCuren, R., Cliff, S.S., Perry, K.D. and Jimenez-Cruz, M. (2005). Asian continental aerosol persistence above the marine boundary layer over the eastern North Pacific: Continuous aerosol measurements form Intercontinental Transport and Chemical Transformation 2002 (ITCT 2K2). *J. Geophys. Res.* 110: D09S90.

Waren, S.G. and Wiscombe, W.J. (1980). A Model for the Special Albedo of Snow. I: Pure Snow. *J. Atmos. Sci.* 37: 2712–2733.

Wulder, M.A., Masek, J.G., Cohen, W.B., Loveland, T.R. and Woodcock, C.E. (2012). Opening the archive: How free data has enabled the science and monitoring promise of Landsat. *Remote Sens. Environ.* 122: 2–10.

Xu, B., Cao, J., Hansen, J., Yao, T., Joswla, D.R., Wang, N., Wu, G., Wang, M., Zhao, H., Yang, W., Liu, X. and He, J. (2009). Black Soot and the Survival of Tibetan Glaciers. *Proc. Natl. Acad. Sci. U.S.A.* 106: 22114–22118.

Zhu, Z. and Woodcock, C.E. (2012). Object-based cloud and cloud shadow detection in Landsat imagery. *Remote Sens. Environ.* 118: 83–94.